19th Australasian Fluid Mechanics Conference
Melbourne, Australia
8-11 December 2014

Macroscopic and Microscopic Characteristics of Ethanol and Gasoline Sprays

Y. Huang[1,2], S. Huang[1], R. Huang[1] and G. Hong[2]

[1] School of Energy and Power Engineering
Huazhong University of Science and Technology, Wuhan, Hubei, 430074, China

[2] School of Electrical, Mechanical and Mechatronic Systems
University of Technology, Sydney (UTS), NSW, 2007, Australia

Abstract

This paper reports the macroscopic and microscopic characteristics of ethanol and gasoline direct injection sprays from a multi-hole injector. The spray experiments were conducted in a constant volume chamber in atmospheric condition (1 bar and 300 K ambient condition). Compressed nitrogen was used to pressurize the injection pressure which was 6.0 MPa. The injection pulse width was 2.0 ms. The high speed Shadowgraphy imaging technique with a speed of 20000 fps @ 608×288 pixels was used to capture the macroscopic spray characteristics. Based on that, the high magnification imaging of the ethanol and gasoline sprays close to the nozzle exit was conducted with the same flash and camera but with an AFTVision ZL0911 microscope. In order to capture the first fuel seen from the nozzle exit, the camera speed was increased to 50000 fps @ 240×88 pixels. Results showed that the macroscopic characteristics of ethanol and gasoline sprays were rather similar in terms of spray tip penetration, spray angle and spray projected area in spite of the differences in physical properties. However, the magnified spray images at the nozzle exit showed that ethanol spray had a larger and sheet-like ligaments at the end of injection than gasoline spray did due to ethanol's larger surface tension and viscosity. It may imply that the fuel properties only have significant effect on the spray during the primary breakup process, but not on the secondary breakup process.

Introduction

Gasoline direct injection (GDI) has several advantages over port fuel injection, including improved fuel economy and transient response, more precise air-fuel ratio control, extended EGR tolerance limit, selective emissions advantages and enhanced potential for system optimization [1]. On the other hand, ethanol is a widely used alternative fuel to address the issue of sustainability. Compared with gasoline fuel, ethanol has greater latent heat of vaporization, larger octane number, higher flame propagation speed and smaller stoichiometric air/fuel ratio. Recently, ethanol direct injection (EDI) has attracted much attention due to its great potential in taking the advantages of ethanol fuel to increase the compression ratio and thermal efficiency [2]. However, the adequate performance of direct injection system is the key factor to achieve the benefits of GDI and EDI.

Compared with gasoline, ethanol has bigger surface tension, viscosity, density, specific heat and enthalpy of vaporisation, but lower vapour pressure. Theoretically, the breakup and evaporation rates of ethanol spray should be lower than that of gasoline spray, thus resulting in a longer spray tip penetration and bigger droplet size. However, experimental results have not reached a consensus. Regarding the spray tip penetration, in spite of the differences in the experiments, gasoline and ethanol gave very similar behaviours [3-6]. On the other hand, some researchers observed that the spray tip penetration decreased with the increase of ethanol fraction [7, 8]. Almost the same spray cone angles were observed for both ethanol and gasoline sprays with high-pressure swirl injector [6]. However experiments in [3, 4, 7] measured larger spray cone angles of ethanol than gasoline's. For spray droplet size, most studies observed that ethanol (or E85) sprays had larger Sauter Mean Diameter (SMD) than gasoline's [4, 6, 9], while the SMD of ethanol and gasoline sprays measured in [3] was very similar in spite of the large differences in viscosity and surface tension.

Although the fuel properties of ethanol are different from that of gasoline, different spray behaviours in theoretical analysis have not been reported in experiments. In the experimental studies as reviewed above, they all focused on the macroscopic characteristics (spray tip penetration, spray angle and droplet size, etc.) of ethanol and gasoline sprays. However the real effect of fuel properties may be on the microscopic spray behaviours, such as primary breakup and evaporation processes. Anand et al. investigated the primary breakup process of ethanol and gasoline sprays from a low-pressure multi-hole port fuel injector [3]. The magnified images at the nozzle exit showed that ethanol spray had larger and thinner sheet-like ligaments than gasoline did. Gasoline near-field spray images of an outward-opening injector revealed the transition in the spray breakup mechanism [10]. The near-nozzle-exit spray characteristics of swirl type injector were also investigated [11, 12]. Recently, the multi-hole injectors have attracted more attention for gasoline direction injection spark ignition (DISI) engines because of their advantages in stability of spray pattern and flexibility of spray plume targeting [13]. However the majority of work published to date on multi-hole injectors concerns diesel nozzles [5].

To better understand the mixture formation process of the EDI and GDI sprays and provide essential data for engine modelling, spray experiments for a high pressure multi-hole injector were conducted on a constant volume chamber. The high speed Shadowgraphy imaging technique was used to capture the macroscopic spray characteristics. Meanwhile the microscopic spray characteristics of the ethanol and gasoline sprays close to the nozzle exit were investigated based on experiments using the high-speed camera and a microscope.

Experiment Apparatus and Procedure

Injector

The injector used in this study was a 6-hole nozzle which was used in experimental investigations to an EDI+GPI research engine [14]. Figure 1 shows the distribution of the nozzle holes on the injector tip and the magnified view of the nozzle exit using a microscope. The measured nozzle diameter was 110 μm. Since the six nozzle holes have different machining angles in the injector, the emanated spray bends to the direction of the injector solenoid valve, as illustrated in figures 2 and 3. The six plumes

are distributed in three groups. The first group contains only one plume whose axis is the same as that of the injector. The second group contains three plumes and the bend angle is 17° to the injector axis. The third group contains two plumes and the bend angle is 34°.

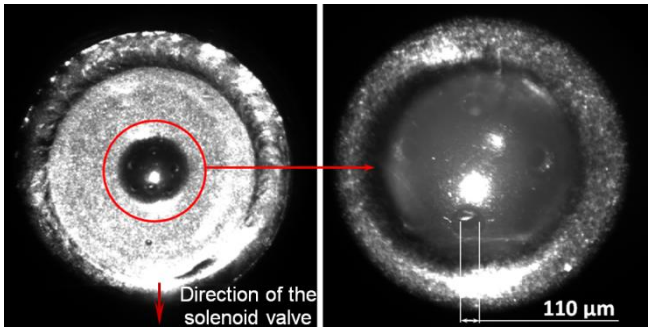

Figure 1. Overall view of the injector tip (left) and magnified view of the nozzle holes (right).

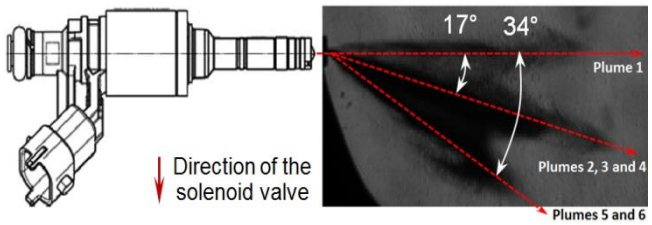

Figure 2. Lateral view of the spray plumes and their directions.

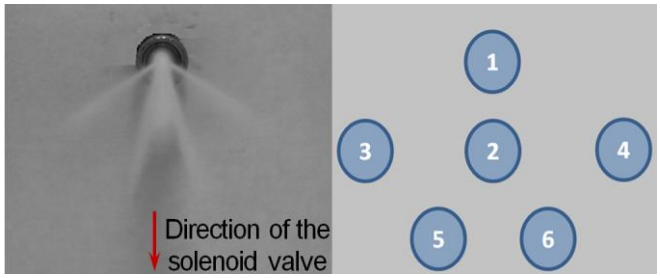

Figure 3. Front view of the spray plumes and their footprints.

Test Fuels

The ethanol fuel investigated in this study was the absolute ethyl alcohol with a purity of 99.9%. The gasoline fuel tested was the commercial unleaded gasoline with an octane number of 97. Table 1 shows the physical properties of ethanol and gasoline fuels at 300 K.

Properties \ Fuel	Ethanol	Gasoline
Chemical formula (-)	C_2H_6O	C_8H_{18}
Density (kg/m^3)	785.5	714.9
Specific heat (J/kg•K)	2339	2041
Viscosity (kg/m•s)	0.001007	0.0004549
Boiling point (K)	351.44	372.39
Diffusion coefficient in air (m^2/s)	1.196×10^{-5}	6.410×10^{-6}
Enthalpy of vaporization (kJ/kg)	948	298
Saturation vapor pressure (kPa)	8.773	28.828
Surface tension (N/m)	0.02314	0.01816

Table 1. Properties of ethanol and gasoline fuels at 300 K.

Experimental Apparatus

Figure 4 is the schematic of the experimental apparatus including the constant volume chamber, the fuel injection system, the Schlieren/Shadowgraphy optical system and the vacuum system. The chamber has a cubic inner length of 136 mm. The diameter of the quartz window is 130 mm.. The injector was mounted horizontally. Its axis was perpendicular to the light pathway. The Shadowgraphy technique was used to visualize the time-resolved spray field (the item 16 knife edge was not used). A nitrogen cylinder was used to pressurize and control the injection pressure. The injection pulse width was generated by a single-chip computer. Meanwhile, the driven signal was sent to trigger the MotionPro Y4S1 high speed CCD camera simultaneously. The high magnification imaging of the ethanol and gasoline sprays close to the nozzle exit was conducted with the same flash and camera but with an AFTVision ZL0911 microscope.

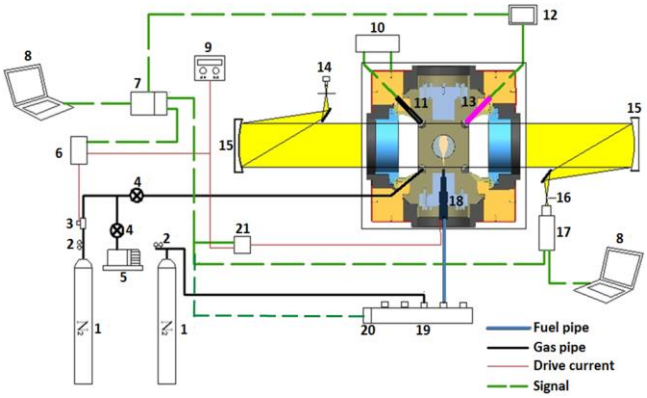

1. High pressure nitrogen cylinder 2. Pressure reducing valve 3. Solenoid valve 4. Hand valve 5. Vacuum pump 6. Solenoid valve control unit 7. NI USB-6251M data acquisition card 8. Computer 9. Power source 10. CVCB temperature control unit 11. Pt100 temperature transducer 12. Kistler 5018 charge amplifier 13. Kistler 6052C pressure transducer 14. Tungsten halogen lamp 15. Reflective mirror 16. Knife edge 17. MotionPro Y4S1 CCD camera 18. Injector 19. High pressure fuel rail 20. Fuel rail pressure sensor 21. Fuel injection control unit

Figure 4. Schematic diagram of the fuel spray experiment apparatus.

Experimental Conditions

The fuel injection pressure was adjusted using the compressed nitrogen at the pressure of 6 MPa. 6 MPa was the direct injection pressure of the ethanol fuel applied in the experiments on the EDI+GPI research engine [14]. The ambient pressure was 1 bar and the ambient temperature was 300 K. The injection duration was held constant at 2 ms. The speed of the macroscopic spray characteristics imaging was 20000 fps @ 608×288 pixels. However, the camera speed was increased to 50000 fps @ 240×88 pixels in order to capture the first fuel seen from the nozzle exit. The measured fuel mass of each injection was 10.844 mg @ 6 MPa × 2 ms for EDI spray and 9.016 mg @ 6 MPa × 2 ms for GDI spray.

Image Processing

The captured images were 8-bit grey scale images. The images were processed using a Matlab code. A threshold of 5% was defined to determine the boundary between the spray area and the background. The macroscopic spray characteristics were calculated based on the spray boundary. Figure 5 shows the definitions for the spray characteristics. The spray tip penetration was defined as the longest distance that the spray travelled. The spray projected area was the area within the spray boundary. The spray angle was defined according to the SAE J2715 Standard. The spray tip penetration, angle and projected area reported in the following sections were the averaged values of five repeated measurements for each spray condition.

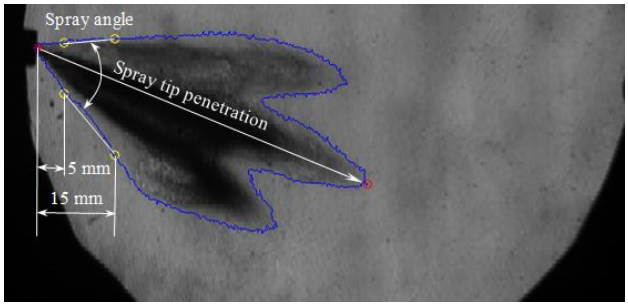

Figure 5. Definitions of the spray characteristics.

Results and Discussion

Macroscopic Spray Characteristics

Figure 6 shows ethanol and gasoline spray patterns varying with time. As shown in figure 6, in general, the spray patterns of ethanol are very similar to that of gasoline. The three plume groups can be clearly identified. The plumes are narrow and plume boundary is smooth. After 4.0 ms after the start of injection (ASOI), the spray droplets lose almost all of their momentum floating at the same position in the chamber. However, the gasoline plumes are slightly wider and the swirl at the tip of the third plume is bigger than ethanol's. This indicates that gasoline fuel spray has a stronger interaction with the ambient gas than ethanol fuel spray does. By the time of 8.0 ms ASOI, the color of the gasoline spray area is slightly lighter than that of ethanol, which indicates a faster evaporation rate of gasoline spray than ethanol spray's. This is because gasoline fuel has complex compositions ranged from C2 to C14. The light components in gasoline evaporate easily and quickly.

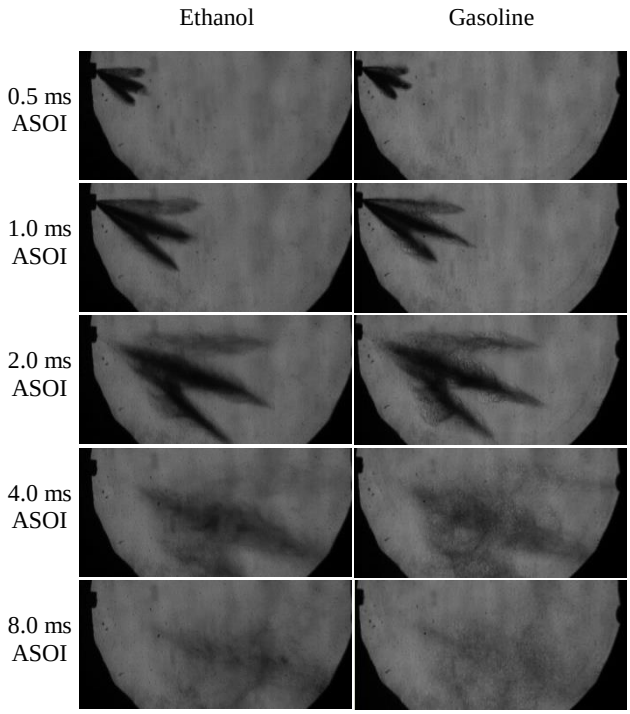

Figure 6. Macroscopic spray images of ethanol and gasoline.

Ethanol and gasoline sprays show very similar macroscopic characteristics in terms of spray tip penetration, spray projected area and spray angle. Figure 7 shows spray tip penetrations of ethanol and gasoline fuels. Before 0.5 ms ASOI, the difference in the penetration length between ethanol and gasoline sprays is negligible. During 0.5-2.5 ms ASOI, the spray tip penetration of gasoline is slightly higher that ethanol's. Finally they reach the similar penetration length after 2.5 ms ASOI. Figure 8 shows the projected areas of ethanol and gasoline sprays. As shown in figure 8, the projected areas of ethanol and gasoline sprays are the same before 3.0 ms ASOI. After that, the gasoline spray area become smaller than ethanol's due to gasoline's faster evaporation rate. Regarding the spray angle, as shown in figure 9, the ethanol has bigger spray angles than gasoline does during 0.8-1.0 ms ASOI. Then they reach similar values of spray angles.

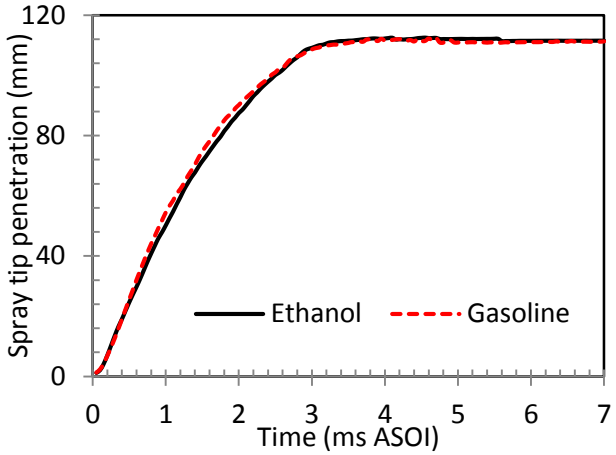

Figure 7. Ethanol and gasoline spray tip penetrations.

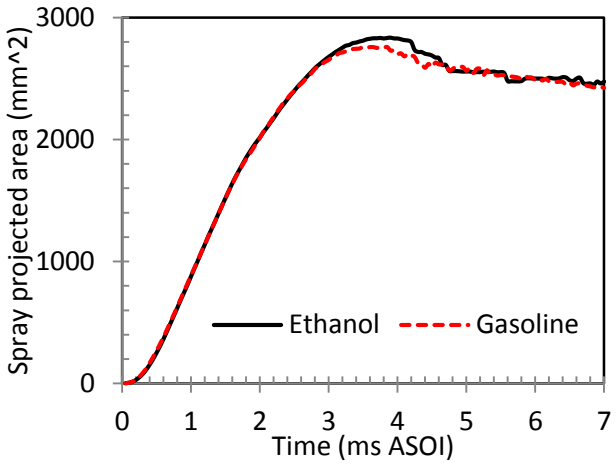

Figure 8. Ethanol and gasoline spray projected areas.

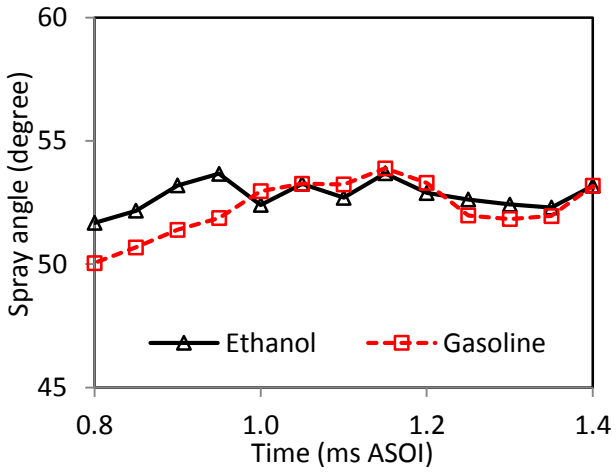

Figure 9. Ethanol and gasoline spray angles.

Microscopic Spray Characteristics

Figure 10 shows the magnified ethanol and gasoline spray images near the nozzle exit. As shown in the images at 0.1 ms ASOI, the very first fuel spray of ethanol shown at the nozzle tip is wider than that of gasoline. During the main injection process

(0.2-1.5 ms ASOI), the spray jets at the nozzle vicinity are similar for ethanol and gasoline fuels. The gasoline spray stops earlier than ethanol does, as shown in the images at 1.6 ms ASOI. At the end of injection (1.8 and 2.0 ms ASOI), it can be seen that ethanol spray has some large and sheet-like ligaments, while the droplets in gasoline spray are much smaller. This is caused by ethanol's larger surface tension and viscosity than gasoline's. As shown in figure 6, significant difference in the macroscopic images of ethanol and gasoline sprays has not been observed. Therefore, it may imply that the fuel properties only have significant effect on the spray during the primary breakup process, but not on the secondary breakup process.

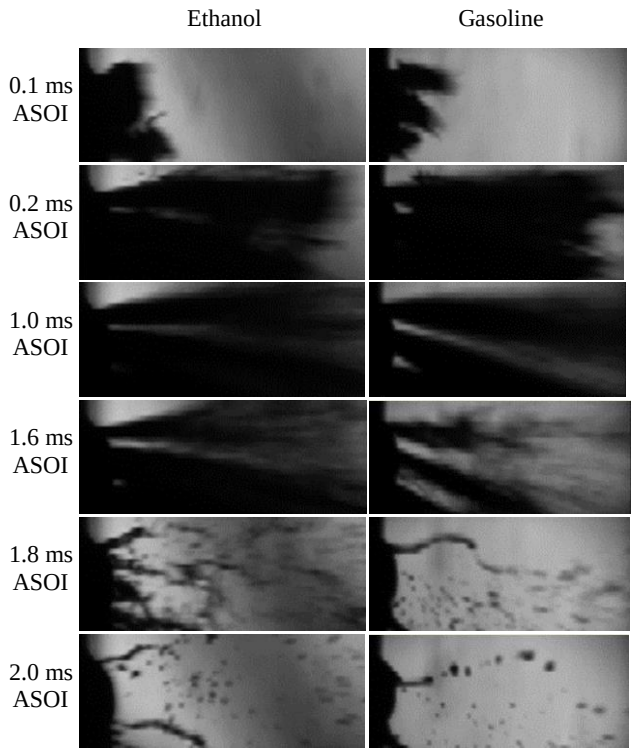

Figure 10. Microscopic spray images of ethanol and gasoline.

Conclusions

The high-speed imaging technique was used to investigate the macroscopic and microscopic characteristics of ethanol and gasoline direct injection sprays. Experiments were conducted in a constant volume chamber in condition of 6.0 MPa injection pressure, 1.0 bar ambient pressure and 300 K ambient temperature. The major results of this study can be concluded as follows:

1. Gasoline fuel spray had a stronger interaction with the ambient gas than ethanol fuel spray did.
2. The macroscopic characteristics of ethanol and gasoline fuel sprays were similar to each other in terms of spray tip penetration, projected area and spray angle.
3. The larger and sheet-like ligaments were found in the ethanol spray at the end of injection due to its greater surface tension and viscosity than gasoline's.
4. Conclusions 2 and 3 may imply that the fuel properties only have significant effect on the spray during the primary breakup process, but not on the secondary breakup process.

Acknowledgements

The scholarship provided by the China Scholarship Council (CSC) is gratefully appreciated. The authors would like to express their great appreciation to Mr. Peng DENG, Mr. Yinjie MA and the workshop at the Huazhong University of Science and Technology (HUST) in China for their technical assistance and support.

References

[1] Zhao, F., Lai, M.C. & Harrington, D.L., Automotive spark-ignited direct-injection gasoline engines, *Progress in Energy and Combustion Science*, 25, 1999, 437-562.

[2] Huang, Y., Hong, G., Cheng, X. & Huang, R. Investigation to Charge Cooling Effect of Evaporation of Ethanol Fuel Directly Injected in a Gasoline Port Injection Engine, *SAE paper 2013-01-2610*, 2013.

[3] Anand, T.N.C., Madan Mohan, A. & Ravikrishna, R.V., Spray characterization of gasoline-ethanol blends from a multi-hole port fuel injector, *Fuel*, 102, 2012, 613-623.

[4] Park, S.H., Kim, H.J., Suh, H.K. & Lee, C.S., Atomization and spray characteristics of bioethanol and bioethanol blended gasoline fuel injected through a direct injection gasoline injector, *International Journal of Heat and Fluid Flow*, 30, 2009, 1183-1192.

[5] Aleiferis, P.G. & van Romunde, Z.R., An analysis of spray development with iso-octane, n-pentane, gasoline, ethanol and n-butanol from a multi-hole injector under hot fuel conditions, *Fuel*, 105, 2013, 143-168.

[6] Wang, X., Gao, J., Jiang, D., Huang, Z. & Chen, W., Spray Characteristics of High-Pressure Swirl Injector Fueled with Methanol and Ethanol, *Energy & Fuels*, 19, 2005, 2394-2401.

[7] Gao, J., Jiang, D. & Huang, Z., Spray Properties of Alternative Fuels: A Comparative Analysis of Ethanol–Gasoline Blends and Gasoline, *Fuel*, 86, 2007, 1645-1650.

[8] Zhu, B., Xu, M., Zhang, Y. & Zhang, G. Physical Properties of Gasoline-Alcohol Blends and Their Influences on Spray Characteristics from a Low Pressure DI Injector, *Proceedings of the 14th Asia Annual Conference on Liquid Atomization and Spray Systems (ILASS-Asia)*, 2010.

[9] Aleiferis, P.G., Serras-Pereira, J., van Romunde, Z., Caine, J. & Wirth, M., Mechanisms of spray formation and combustion from a multi-hole injector with E85 and gasoline, *Combustion and Flame*, 157, 2010, 735-756.

[10] Befrui, B., Corbinelli, G., Robart, D., Reckers, W. & Weller, H. LES Simulation of the Internal Flow and Near-Field Spray Structure of an Outward-Opening GDi Injector and Comparison with Imaging Data, *SAE paper 2008-01-0137*, 2008.

[11] Kawahara, N., Tomita, E., Kasahara, D., Nakayama, T. & Sumida, M. Fuel Breakup Near Nozzle Exit of High-Pressure Swirl Injector for Gasoline Direct Injection Engine, *SAE paper 2004-01-0542*, 2004.

[12] Wigley, G., Goodwin, M.S. & Pitcher, G. Temporal Analysis of the Fuel Breakup and Atomisation in the Near Nozzle Region of a GDI Injector, *SAE paper 2003-01-1800*, 2003.

[13] Matsumoto, A., Zheng, Y., Xie, X.-B., Lai, M.-C. & Moore, W. Characterization of Multi-hole Spray and Mixing of Ethanol and Gasoline Fuels under DI Engine Conditions, *SAE paper 2010-01-2151*, 2010.

[14] Zhuang, Y. & Hong, G., Primary Investigation to Leveraging Effect of Using Ethanol Fuel on Reducing Gasoline Fuel Consumption, *Fuel*, 105, 2013, 425-431.